Acid−Base Equilibria in 5,10,15,20-Tetrakis(4-sulfonatophenyl)chlorin: Role of Conformational Flexibility

Mikalai M. Kruk[†,‡] and Silvia E. Braslavsky*[,‡]

Institute of Molecular and Atomic Physics of National Academy of Sciences, 70 F. Skaryna Avenue, 2202072 Mink, Belarus, and Max-Planck-Institut für Bioanorganische Chemie, Postfach 101365, D-45413 Mülheim an der Ruhr, Germany

Received: November 28, 2005; In Final Form: January 23, 2006

The acid−base equilibria in 5,10,15,20-tetrakis(4-sulfonatophenyl)chlorin were studied in aqueous solution and compared with the respective data for the corresponding porphyrin. The reduction of the pyrrole ring in the tetrapyrrolic macrocycle noticeably influences both free base/monoprotonated and mono-/diprotonated species equilibria. In strong acidic solutions protonation of 4-sulfonatophenyl groups takes place in addition to protonation of the macrocycle core. The photophysical properties of all ionic forms are influenced by an enhanced rate of internal $S_1 \rightarrow S_0$ conversion, leading to about 50% and 90% deactivation through this channel for the free base and diprotonated species, respectively. The enhancement of the rate of the radiationless transitions is explained by an increased conformational flexibility of the chlorin macrocycle with respect to that of a porphyrin. Structural volume change measurements with laser-induced optoacoustic spectroscopy support this explanation. The contraction upon triplet state formation of the free base is about one-half of that measured for the corresponding porphyrin. This contraction should be due to intramolecular structural rearrangements of the macrocycle to adopt a minimum energy conformation in case of the chlorin. On the contrary, for the more rigid porphyrin macrocycle the interactions of the molecule with the solvent environment play a more important role. The diprotonated forms of both porphyrin and chlorin show a high radiationless $S_1 \rightarrow S_0$ conversion rate and seem to have a similar conformational flexibility. In agreement with previous calculations, the conformational flexibility of the diprotonated forms appears to be higher than that of the free base molecule.

Introduction

Selective accumulation of photosensitizer molecules in malignant tissues is at the basis of photodynamic therapy.[1,2] Although the exact nature and the mechanism(s) responsible for the selective uptake and retention of tetrapyrrolic photosensitizers are not completely understood, there is mounting evidence that the physiology of the whole tumor must be considered rather than some special property of the malignant cells.[1] The pH value of several rapidly growing tumors is often found to be substantially lower than that of normal tissue in the same individual. In tumor tissue, the microvasculature is substantially altered, leading to a reduced blood flow. This causes tumor cells to undergo anaerobic glycolysis, producing large quantities of lactic acid.[3] Correlations between lactic acid content and interstitial pH have been revealed in many tumors.[4] Lower extracellular pH in tumors compared to that in normal tissues is expected to be one of the factors contributing to the tumor selective uptake of several photosensitizers.[5−7] In addition to the tumor tissue properties, the nature of the photosensitizer should be taken into account, since distribution and cellular uptake depend strongly on physicochemical properties of the photosensitizer such as molecular structure, size, charge distribution, and solubility.[2] Thus, even small changes in the pH of tissue can shift the acid−base equilibria between the various photosensitizer ionic species. Acid−base equilibria shifts in the photosensitizer molecule can vary its physicochemical properties such as aggregation state, net charge, and lipophilicity. Formation of protonated species is accompanied by increase in the lipophilicity of the molecule, which in turn leads to higher cellular uptake.

The influence of the interstitial and cellular pH on the selective distribution and uptake of the tetrapyrrolic photosensitizers was the subject of numerous studies (refs 1, 5, 7 and references therein), whereas the role of acid−base equilibria in the photophysical properties of the photosensitizer has received less attention. Several papers are known in this field,[8−15] but a detailed understanding is lacking of the role of acid−base equilibria in the rearrangement of the photosensitizer structure, in the possible changes in rate constants of intramolecular processes such as fluorescence, internal conversion, and intersystem crossing, and in the modulation of solute−solvent interactions.

Tetrapyrrolic macrocycles undergo several protonation steps involving both pyrrolenic (−N=) and pyrrolic (−NH−) nitrogens.[16] The peripherical substituent groups can also be involved in the acid−base equilibria in addition to those of the macrocycle itself. So far, acid−base equilibrium studies for tetrapyrrolic compounds have been mainly focused on the protonation of the macrocycle core, whereas acid−base equilibria for peripherical substituents were not thoroughly considered. Tetraaryl-substituted porphyrins have received much less attention than,

* Author to whom correspondence should be addressed. Fax: +49 (208) 306 3681. E-mail: braslavskys@mpi-muelheim.mpg.de.

† Institute of Molecular and Atomic Physics of National Academy of Sciences.

‡ Max-Planck-Institut für Bioanorganische Chemie (formerly Strahlenchemie).

10.1021/jp056896h CCC: $33.50
Published on Web 02/23/2006

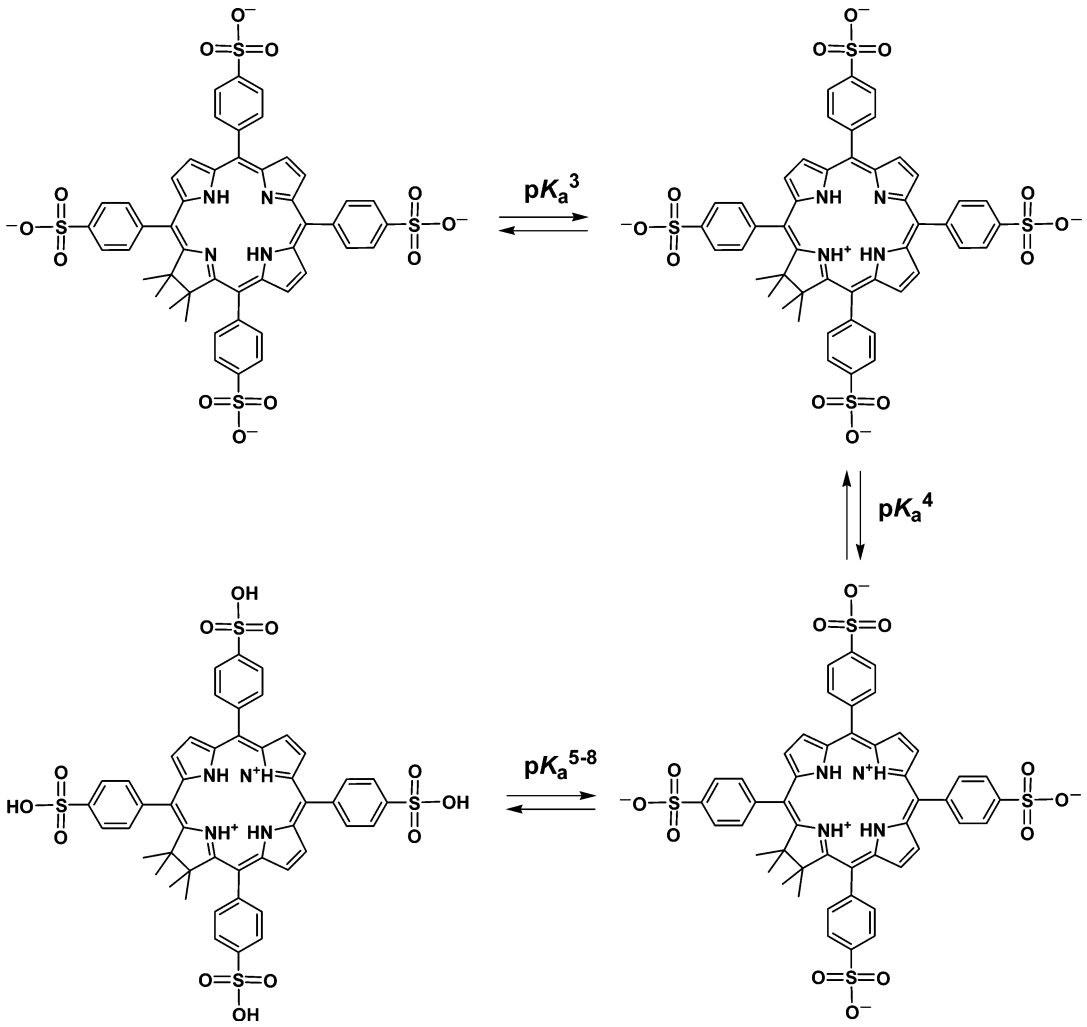

Figure 1. Acid−base equilibria in 5,10,15,20-tetrakis(4-sulfonatophenyl)chlorin.

e.g., hematoporphyrin IX (see refs 10, 11, 17) or deuteroporphyrin[18] and its disulfonated derivative.[11]

In this paper we present the results of a study on the acid−base equilibria in 5,10,15,20-tetrakis(4-sulfonatophenyl)chlorin ($TSPC^{4-}$) in aqueous solutions (Figure 1). The present work is a continuation of the studies of acid−base equilibria in a series of tetra-*meso*-aryl-substituted tetrapyrrolic compounds.[19] In the preceding paper the equilibrium between the free base (FB) and the mono- and diprotonated (MP and DP) forms of 5,10,15,20-tetrakis(4-sulfonatophenyl)porphine ($TSPP^{4-}$) was described. Special attention was given to the question of how changes in the *meso*-aryl-substituent structure influence the solute−solvent interactions as detected by laser-induced optoacoustic spectroscopy (LIOAS). It was shown that the substituents' variations barely affect the value of the structural volume change upon triplet state formation, $\Delta_T V$. A contraction, i.e., $\Delta_T V = 16-18$ Å^3 and $4-5$ Å^3 upon triplet state formation of FB and DP forms, respectively, was measured for all the *meso*-phenyl substituted porphyrins.[19] These contractions were proposed to be due to water rearrangement in case of the FBs, whereas they should be intrinsic to changes in the macrocycle in the case of the DP forms, as well as in the case of the porphyrin Zn complexes.

Here we report on the analogies and differences in the acid−base equilibria between $TSPC^{4-}$ and its porphyrin counterpart, $TSPP^{4-}$. The pK_a values derived from absorption and fluorescence titrations show a considerable influence of the reduction of the pyrrole ring. The additional protonation of the 4-sulfonatophenyl group results in noticeable changes of both absorbance and fluorescence properties at strong acidic pH. Radiationless internal $S_1 \rightarrow S_0$ conversion plays a major role in the deactivation of the excited species. The values of $\Delta_T V$, as measured by LIOAS, indicate that these structural alterations in the tetrapyrrolic macrocycle have substantial influence on solute−solvent interactions. The data are analyzed within the framework of variations of the macrocycle conformational flexibility.

Experimental Section

Chemicals. 5,10,15,20-Tetrakis(4-sulfonatophenyl)chlorin ($TSPC^{4-}$) was prepared by diimide reduction of the corresponding porphyrin as reported.[20] 5,10,15,20-Tetrakis(4-sulfonatophenyl)porphine ($TSPP^{4-}$) was purchased from Porphyrin Products (Logan, UT) and used as received. Evans blue (EB) was from Aldrich (Deisenhofer), and bromocresol purple (5,5′-dibromo-*o*-cresol-sulfonaphthalene, BCP) was from Fluka (Buchs, Switzerland). Water was purified with a Millipore Milli-Q Water System.

Solutions. The solutions were prepared in air-equilibrated 100 mM Na acetate buffer, and the pH value was adjusted with 0.1−2 M HCl solutions. All experiments were at 20 ± 2 °C unless otherwise stated. The working concentrations were in the range 0.1−30 μM for absorbance measurements, 2.5−30 μM for steady-state and time-resolved fluorescence, 4−5 μM for transient triplet−triplet absorbance and singlet oxygen phosphorescence, and 10 μM for LIOAS experiments. Absorp-

tion spectra were taken with a UV-2102 spectrophotometer (Shimadzu). For LIOAS experiments both sample and reference solutions were dissolved in the same buffer and matched in absorbance at the excitation wavelength, $A(532) = 0.06-0.10$ (± 0.005), depending on the solution. For the measurements of the fluorescence quantum yield, Φ_F, and the quantum yield of singlet molecular oxygen [$O_2(^1\Delta_g)$] production, Φ_Δ, the absorbance of the solutions at λ(exc) was $A(540) = 0.10-0.12$ and $A(532) = 0.14-0.26$, respectively. The signals were normalized for the fraction of light absorbed $f = 1 - 10^{-A_{exc}}$, where A_{exc} is the absorbance at λ(exc).

All measurements were carried out in air-equilibrated solutions with the exception of the Φ_F determinations, for which the solutions were bubbled with Ar for 20 min just before the experiments.

Emission and Transient Absorption Data. Steady-state fluorescence spectra were recorded with Spex Fluorolog equipment as described.[21] Time-resolved fluorescence was measured with a single photon counting system (FLA 900, Edinburgh Instruments, U.K.). Time-resolved phosphorescence of $O_2(^1\Delta_g)$ by its near-infrared emission at 1270 nm was detected with a liquid-nitrogen cooled Ge detector (EO817FP, North Coast) as described earlier.[22,23] $TSPP^{4-}$ ($\Phi_F = 0.06$ at <30 mm and pH = 7.8[24] and $\Phi_\Delta = 0.62$[19]) was used as the reference compound.

Transient triplet−triplet absorption measurements were performed with home-built laser flash photolysis equipment using the second harmonic of a Nd:YAG laser (JK Lasers, Rugby, U.K., 11 ns pulses) as the laser source.[25]

LIOAS. The setup for laser-induced optoacoustic spectroscopy (LIOAS) has been described in several publications (refs 19, 24, 26 and references therein). The second harmonic (532 nm) of a Q-switched Nd:YAG laser (Spectron Lasers, Rugby, U.K., 8 ns pulses) was used as excitation source. The beam was shaped by a slit (1.0 mm width) in front of the cuvette. All experiments were performed with low photon fluence providing at most excitation of 15% of the molecules within the excited volume. The linearity of the LIOAS signal with excitation energy was tested before the measurements. Bromocresol purple (BCP) and Evans blue (EB) were used as the calorimetric references providing the instrumental function for deconvolution.[27] The ratio of thermoelastic parameters ($c_p\rho/\beta$) of the solutions (with c_p the specific heat capacity, ρ the mass density, and β the thermal expansion coefficient) was determined for the range 10−25 °C, by a comparative method using BCP as calorimetric reference in the buffered solution and EB in neat water. The data for the buffer were thus obtained using the equations already presented and the literature values for water.[28] The structural volume changes were determined by applying the several temperatures (ST) method[24,26] and eq 1,

$$\varphi_i = \alpha_i + \frac{\Phi_i \Delta_i V}{E_\lambda}\left(\frac{c_p\rho}{\beta}\right)_T \qquad (1)$$

where φ_i is the amplitude of each of the single-exponential components of the multiexponential function describing the time evolution of the pressure wave after excitation, $\alpha_i = q_i/E_\lambda$ is the fraction of absorbed energy emitted as heat during the process i, Φ_i and $\Delta_i V$ are the quantum yield and the structural volume change for process i, and E_λ is the molar energy of the laser pulse.

The LIOAS signal handling has been extensively described in several articles.[19,24,26,29−32] The triplet state lifetimes measured by transient absorbance are more precise than those obtained by deconvolution of the LIOAS signals due to the strong correlation between the lifetimes and the amplitudes in the latter method. Thus, for the analysis of the LIOAS experiments, the triplet lifetime was fixed to the values measured by transient absorbance in order to obtain higher precision in the amplitude values (eq 1) derived from deconvolution.[31]

Results and Discussion

Absorption Spectra. Prior to measuring of the pH dependence of the absorption and fluorescence spectra, the solutions were checked for the presence of aggregates. It is known that dimer formation (as a first step in the aggregation processes) induces a red shift of all the visible bands with the $Q_x(0,0)$ band shifting more than the $Q_y(0,0)$ band. Therefore, the $Q_x(0,0)$ band strongly overlaps with the vibronic $Q_y(0,1)$ band and one of the four Q-bands "disappears".[33] No spectral evidence of dimer formation was found for the samples with chlorin concentration from 0.1 to 30 μM in 100 mM Na-acetate-HCl buffer in the whole pH and temperature ranges. The temperature factor was taken into account since the aggregation of water-soluble tetrapyrrolic compounds is strongly temperature dependent.[33]

Figure 2 depicts the absorption spectra of 4.1 μM solutions in the 2.0−7.0 pH range. The maximum of the Soret band at 413 nm in neutral solution shifts to 434 nm upon acidification. The positions of the maxima of the Soret and Q-bands in the FB forms of tetra-*meso*-aryl substituted chlorins are very close to those for the corresponding porphyrins.[20,34]

The most pronounced difference in the absorption spectra for this group of porphyrins and chlorins is the increased absorbance of the Q_y-band in chlorin derivatives. The visible absorption spectrum of FB $TSPC^{4-}$ consists of four bands centered at 516, 550, 575, and 645 nm. Upon acidification, the spectrum gradually transforms into a two band spectrum peaking at 579 and 642 nm (characteristic of DP H_2TSPC^{2-}).

The spectral changes are complex. No isobestic points are found in the whole spectral range studied. This indicates that more than two (i.e., FB $TSPC^{4-}$ and DP H_2TSPC^{2-}) species coexist in solution. A third (most probably the monoprotonated, MP, $HTSPC^{3-}$) species should be considered. Clear evidence of the presence of the MP species is found by monitoring the absorbance changes at 645 nm (Figure 3 d; details of the fitting procedure are given below).

Upon decreasing pH from 7 to 5, the absorbance at 645 nm decreases, but upon a further fall of pH an absorbance increase is observed. Thus, from neutral to acidic solutions the MP species is initially formed, leading to the decrease in $A(645)$. Further acidification induces formation of DP species with a higher absorption coefficient at this wavelength, accounting for the increase in $A(645)$.

In strong acidic solution (pH < 2.5) an additional equilibrium seems to appear. The spectral changes in this pH range are clearly visible at several wavelengths within the Q-band region (Figure 3c,d). The absorbance changes either accelerate (585 and 610 nm) or reverse the trend (515 nm). This fact complicates the analysis of the spectral changes in terms of three species because all of them are present in this pH range and all of them could be considered to undergo an additional protonation.

The spectral changes associated with the additional protonation step(s) are relatively small. This is due to the small concentration of this further protonated species or/and to few changes introduced by the locus of proton attachment at the periphery of the macrocycle. We suggest that the new species results from protonation of a SO_3^- group in the *para*-position of the phenyl ring. The spectral changes in such a case will be small, since there is no conjugation between the chlorin

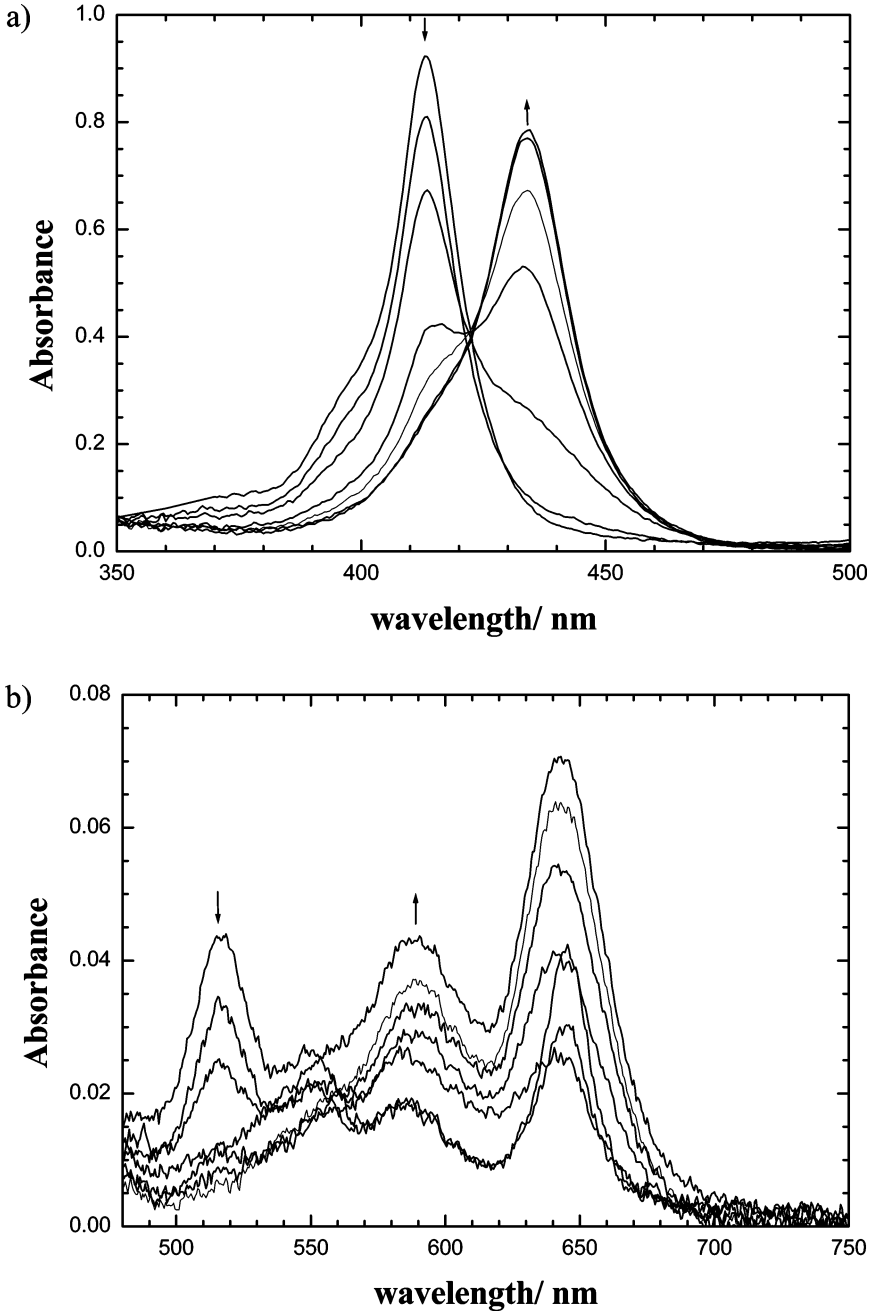

Figure 2. Absorption spectra of 5,10,15,20-tetrakis(4-sulfonatophenyl)chlorin as a function pH: (a) Soret band; (b) Q-bands. Concentration is 4.1 μM. Arrows indicate direction of spectral changes upon going from pH = 7.0 to pH = 2.0.

macrocycle and the phenyl rings. The dihedral angle between the macrocycle plane and the benzene ring is about 27° in the DP species.[35] The limited pH range did not allow an accurate determination of this pK_a. A value pK_a = 1.5 ± 1.5 was estimated. In spite of the large uncertainty in this estimation, one may argue that the value is close to pK_a = 0.7, known for the dissociation of the sulfobenzene acid ($C_6H_5SO_3H$).[36] This supports the idea that the transition $SO_3^- + H^+ \rightleftarrows SO_3H$ in the sulfonatophenyl substituents accounts for the spectral changes found in the strong acid pH range.

It is known that additional spectral changes appear for the corresponding porphyrin $TSPP^{4-}$ in concentrated H_2SO_4 (94 wt %). The moderate (~10 nm) bathochromic shifts of the Q-bands now determined are of the same order of magnitude as those found for both FB and DP forms of water-soluble porphyrins and chlorins upon going from water to ethanol where counterions associate with their parent ionized groups (11.5 and 6 nm for $TSPP^{4-}$ and H_2TSPP^{2-}, respectively).[37] It is likely that association of the SO_3^- groups with Na^+ ions, or their protonation, leads to the same kind of spectral changes. The electron withdrawing character of the SO_3^- group (Hammett constant $\sigma_p > 0$) facilitates protonation as well as association with cations.

An alternative explanation would be protonation in the β-positions of the pyrrole ring. However, $TSPP^{4-}$, as well as several other FB TPP compounds bearing electron withdrawing substituents in the phenyl ring *para*-position, do not show any evidences of formation of proton adducts in the β-positions of the pyrrole ring.[38] Bathochromic shifts up to 70 nm are characteristic for the latter type of adducts, and this large shift was not found upon pH decrease in H_2TSPC^{2-} solutions.

Steady-State Fluorescence. Steady-state fluorescence spectra were measured in the pH range 1.5−7.4 (Figure 4). The fluorescence spectrum undergoes dramatic changes of both

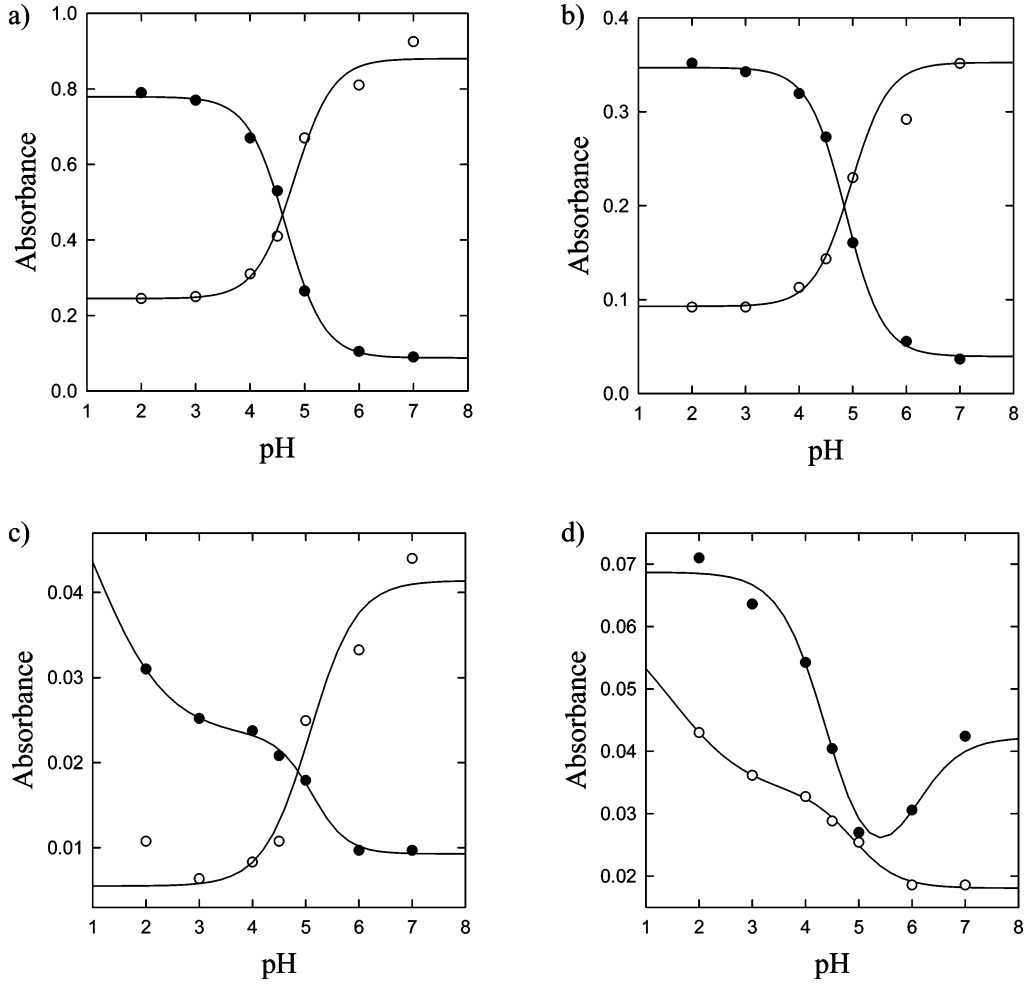

Figure 3. Absorption titration curves: (a) $\lambda = 413$ (○) and 434 nm (●); (b) $\lambda = 400$ (○) and 445 nm (●); (c) $\lambda = 515$ (○) and 610 nm (●); (d) $\lambda = 585$ (○) and 645 nm (●).

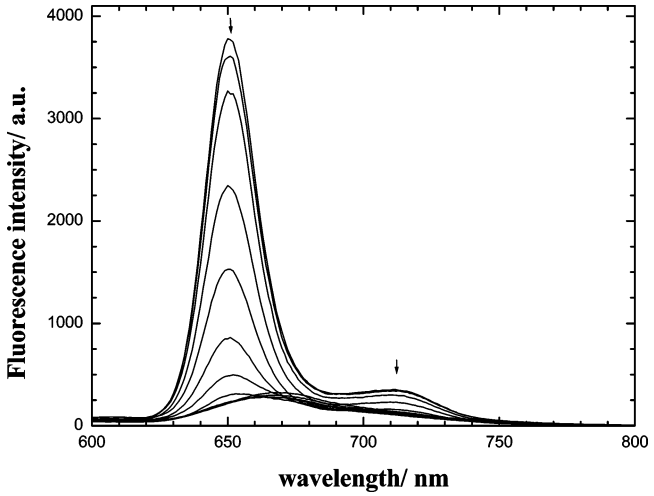

Figure 4. Absorbance-normalized fluorescence spectra of 5,10,15,20-tetrakis(4-sulfonatophenyl)chlorin as a function pH. Concentration is 5.5 μM. Arrows indicate direction of spectral changes upon going from pH = 7.4 to pH = 1.5.

shape and intensity upon acidification. The FB $TSPC^{4-}$ emission spectrum has two peaks at 650 and 712 nm, whereas DP H_2TSPC^{2-} has a broadened one-band fluorescence spectrum with maximum around 668 nm. In the whole pH range no isoemissive points were found. This again indicates that more than two species in equilibrium should be considered and contribution of the MP form should not be neglected. Decrease of the fluorescence intensity at low pH indicates that both the MP and DP forms have a smaller Φ_F than the FB form. A smooth fall of the fluorescence intensity upon pH decrease and the absence of changes in the fluorescence spectrum shape at pH down to 4.5, where a detectable amount of $HTSPC^{3-}$ molecules already exist, indicate that Φ_F for $HTSPC^{3-}$ is $<\Phi_F$ for H_2TSPC^{2-}. $\Phi_F = 0.086$ was calculated at pH = 7.4 for $TSPC^{4-}$ by using the absorbance-normalized integrated emission intensity. At pH 2.5, where the majority of the emissive species are H_2TSPC^{2-}, Φ_F as low as 0.015 was measured. The opposite trend was observed in the corresponding porphyrin $TSPP^{4-}$ where the DP species has a higher Φ_F than the FB.[19,24]

Time-Resolved Fluorescence. The fluorescence decay was faster at low than at high pH at all wavelengths studied. Each decay kinetics was well fitted with a sum of single-exponential decay functions. Global analysis of the decays at various pH values using a three-exponential fitting function and the separate fitting of fluorescence decays at each single pH gave consistent results. At all pH values three species were present, except for extreme alkaline and acid pHs (Figure 5).

The individual lifetimes $\tau_1 = 8.5$ ns, $\tau_2 = 0.5$ ns, and $\tau_3 = 3.5$ ns were unaffected by pH changes. At pH > 7.0 only one decay was observed with $\tau_1 = 8.5$ ns. Thus, τ_1 is assigned to FB $TSPC^{4-}$. A decrease in pH leads to appearance of decay components with lifetimes $\tau_2 = 0.5$ ns and $\tau_3 = 3.5$ ns. At pH = 4.0 the relative amplitude A_3 (lifetime $\tau_3 = 3.5$ ns) is about 40%, whereas the shortest component amplitude, A_2, is <10%. Therefore, $\tau_3 = 3.5$ ns is likely to belong to DP H_2TSPC^{2-}. A

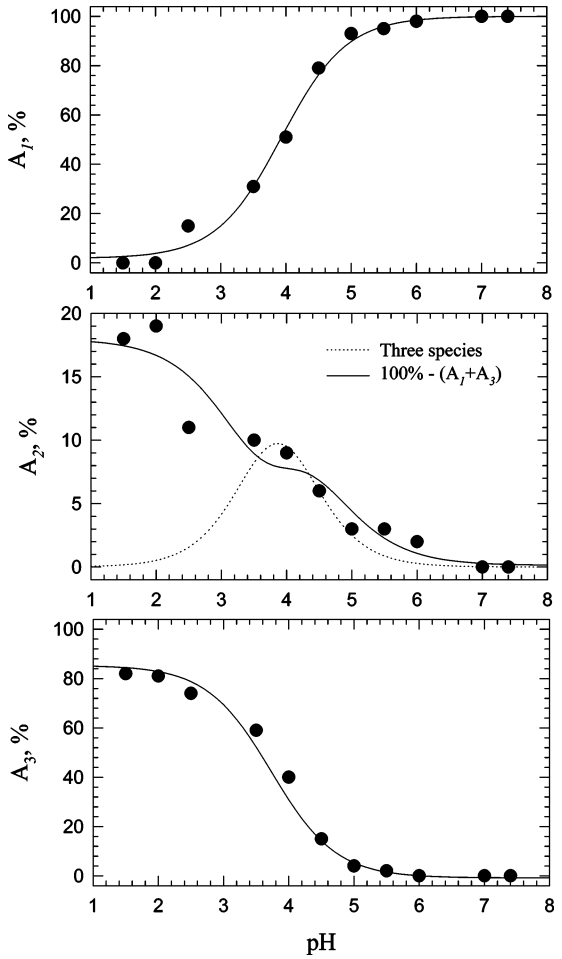

Figure 5. Plots of amplitudes A_i of the fluorescence decay curve components as a function of pH.

minor quantity of the shortest component ($\tau_2 = 0.5$ ns) indicates the presence of MP $HTSPC^{3-}$ molecules.

Support for the interpretation above arises from the comparison with the corresponding porphyrin, for which a longer component of 3.4 ns due to DP H_2TSPP^{2-} was found whereas the shortest component ($\tau = 1.3$ ns) was assigned to MP $HTSPP^{3-}$.[19] However, in the present case, even in strong acidic solution both these components ($\tau_2 = 0.5$ ns and $\tau_3 = 3.5$ ns) coexist and none of them reach 100% weight.

The possibility of aggregation in acidic solution is ruled out since 10-fold dilution at pH = 1.5 does not affect the relative weight of the fluorescence components. Should no other species be in solution, the relative amplitude A_3 should reach 100% and a pH dependence of A_2 would have a bell-like shape. However, the pH dependence of A_2 bears the features of two protonation steps (Figure 5). The A_2 value upon acidification to pH $\sim$ 4.0 reflects the equilibria of the three species.

Upon further pH decrease, A_2 is likely to reflect the species appearing on further protonation found in absorbance and steady-state fluorescence titrations. Since the pK_a value for this transition ($SO_3^- + H^+ \rightleftarrows SO_3H$) < p$K_a^3$ for the formation of the DP species, in strong acidic solutions the decay component with lifetime $\tau_2 = 0.5$ ns arises from DP H_2TSPC^{2-} with additionally protonated SO_3^- group(s) rather than from MP $HTSPC^{3-}$ species. This means that we deal with an accidental coincidence of the fluorescence lifetimes (within the error of the measurements) of these molecular species.

Acid−Base Equilibria. The titration curves measured for $TSPC^{4-}$ reflect three sets of acid−base equilibria: (a) $TSPC^{4-} \rightleftarrows HTSPC^{3-}$ equilibrium; (b) $TSPC^{3-} \rightleftarrows H_2TSPC^{2-}$ equilibrium; and (c) $SO_3^- + H^+ \rightleftarrows SO_3H$, i.e., equilibrium in the sulfonatophenyl substituents of the macrocycle. The latter appears in strong acidic medium and only slightly overlaps with those involving both pyrrolenic (−N═) nitrogens.

On the contrary, the pK_a values for the $TSPC^{4-} \rightleftarrows HTSPC^{3-}$ and $HTSPC^{3-} \rightleftarrows H_2TSPC^{2-}$ equilibria should not be very separated. They usually differ by no more than 2 pH units.[8,10,11,16] This typical picture for tetrapyrrolic compounds complicates the analysis of acid−base equilibria since a lower number of inflection points than expected is observed in titration curves when the pK_a values are separated by less than 2 units,[10,11] i.e., discrimination between pK_a values for two separate FB/MP and MP/DP equilibria is difficult. In fact, the highest possible concentration of MP species varies strongly with $\Delta pK_a = pK_a^3 - pK_a^4$.[39] Thus, if two protonation steps are separated by 4 pH units, the maximum relative concentration of MP species reached at pH = (1/2)(pK_a^3 + pK_a^4) is 98%, whereas for $\Delta pK_a = 1$ this value falls to about 61%.[39]

The Henderson−Hasselbalch eq 2[40] was used for the analysis of the titration curves,

$$a = a_{min} + (a_{med} - a_{min})\frac{1}{10^{n_1(pK_1 - pH)} + 1} + (a_{max} - a_{med})\frac{1}{10^{n_2(pK_2 - pH)} + 1} \quad (2)$$

where a is the observable (i.e., absorbance, fluorescence intensity, etc.); a_{max}, a_{med}, and a_{min} refer to the species at high, intermediate, and low pH, respectively; pK_1 and n_1 and pK_2 and n_2 are pK_a values and Hill indices for two equilibria, respectively, and have their usual meaning.

Absorbance titration curves measured within both the Soret and the visible bands regions are presented in Figure 3. For all wavelengths (with the exception of 645 nm) the absorbance changes for two sequential FB/MP and MP/DP equilibria follow the same direction, i.e., absorbance either decreases (400, 413, 515 nm) or increases (434, 445, 585, 610 nm). Absorbance changes reveal only one inflection point rather than two, indicating that ΔpK_a is rather small. At 645 nm the absorbance initially falls upon pH decrease and then increases manifesting the formation of DP species possessing higher absorbance than the FB and MP molecules.

The absorbance titration curves fitted with eq 2 failed to resolve the pK_a values for the two protonation steps. The average values 4.95 ± 0.15 are overall p$K_a^{3,4}$ for two protonation transitions (Table 1). Positive Hill indices n =1.0−1.36 indicate that more than one proton equilibrium is involved. The distinctly lower value 4.4 ± 0.2 at 645 nm indicates that at 645 nm mostly the equilibrium between MP and DP molecules is monitored. The value should be assigned to pK_a^4 rather than to p$K_a^{3,4}$ averaged over two protonation steps.

A different approach was used to obtain independently pK_a^3 and pK_a^4 (Figure 6). Only the absorbance changes for pH in alkaline and acidic extremes at two individual wavelengths λ_1 and λ_2 were used.[39] In these pH extremes the solution contains mostly two species (FB and MP molecules at alkaline pH, and MP and DP at acidic pH). Consequently, absorbance changes at λ_1 and λ_2 taken in narrow pH intervals at alkaline and acidic extremes should be inversely proportional to each other and reflect the two FB/MP and MP/DP equilibria, respectively.

The intersection of two extrapolated lines in the plot of $A(\lambda_1)$ vs $A(\lambda_2)$ (Figure 6a) gives (albeit with a large uncertainty) the value of A^{MP} at λ_1. The values $A(\lambda_1) = (1/2)(A^{FB} + A^{MP})$ and

TABLE 1: pK_a Values and Hill Indices (Eq 2) for Acid−Base Equilibria in 5,10,15,20-Tetrakis(4-sulfonatophenyl)chlorin

titration technique	pK_a	n
	Absorption	
single λ at 400 nm	$pK_a^{3,4} = 5.0 \pm 0.1$	1.24 ± 0.10
	$pK_a^3 = 5.7 \pm 0.2$, $pK_a^4 = 4.8 \pm 0.2$	
413 nm	$pK_a^{3,4} = 4.9 \pm 0.1$	1.36 ± 0.10
	$pK_a^3 = 5.5 \pm 0.2$, $pK_a^4 = 4.6 \pm 0.2$	
434 nm	$pK_a^{3,4} = 4.7 \pm 0.1$	1.25 ± 0.10
	$pK_a^3 = 5.6 \pm 0.2$, $pK_a^4 = 4.5 \pm 0.2$	
445 nm	$pK_a^{3,4} = 4.9 \pm 0.1$	1.26 ± 0.10
	$pK_a^3 = 5.5 \pm 0.2$, $pK_a^4 = 4.6 \pm 0.2$	
515 nm	$pK_a^{3,4} = 5.1 \pm 0.2$	0.80 ± 0.10
585 nm	$pK_a^{3,4} = 4.9 \pm 0.2$	1.04 ± 0.10
610 nm	$pK_a^{3,4} = 5.1 \pm 0.2$	1.34 ± 0.10
645 nm	$pK_a^4 = 4.4 \pm 0.2$	1.00 ± 0.10
	Fluorescence	
single λ at 650 nm	$pK_a^3 = 5.3 \pm 0.1$	0.91 ± 0.10
715 nm	$pK_a^3 = 5.5 \pm 0.1$	1.15 ± 0.10
Φ_F	$pK_a^3 = 5.4 \pm 0.1$	1.00 ± 0.10
λ_{max}	$pK_a^4 = 3.2 \pm 0.1$	1.15 ± 0.10
decay at λ_{em} = 650 nm	$pK_a^3 = 3.9 \pm 0.2$, $pK_a^4 = 3.7 \pm 0.2$	0.87 ± 0.10, 0.88 ± 0.10

$A(\lambda_1) = (1/2)(A^{DP} + A^{MP})$ correspond to pK_a^3 and pK_a^4, respectively. The pK_a^3 and pK_a^4 are the pH values corresponding to these $A(\lambda_1)$ values from the plot of $A(\lambda_1)$ vs pH (Figure 6b).

This method was applied to four titration curves in the Soret band region, and the resulting pK_a^3 and pK_a^4 values are listed in Table 1. The averages over four wavelengths are p$K_a^3 = 5.6 \pm 0.1$ and p$K_a^4 = 4.6 \pm 0.1$. The latter is in good agreement with p$K_a^4 = 4.4 \pm 0.2$ determined from the absorbance titration curve at 645 nm. A value of $\Delta pK_a = 1$ indicates that the maximum relative amount of MP species is about 61% at pH = 5.1. An inflection point is observed within experimental uncertainty at a pH corresponding to the average p$K_a^{3,4}$ (Figure 3, all traces except $\lambda = 645$ nm).

Fluorescence titration curves mainly reflect disappearance of FB species (Figure 7a,b). This is due to the almost six times larger Φ_F for FB than for the protonated molecules and due to the strong overlap of the fluorescence spectra of all three species. A pattern of the titration curve similar to that obtained through absorbance titration was observed for Φ_F (Figure 7c). As already stated, the small increase in Φ_F at low pH is due to additional protonation at the periphery of the macrocycle and does not affect the acid−base equilibrium in the macrocycle core. The only inflection point found corresponded to that found also during absorbance titrations. The absence of isoemissive points made the evaluations difficult. The low fluorescence intensity of the protonated species was at the basis of the large data scatter.

Fitting of all these data with eq 2 resulted in an average p$K_a^{3,4} = 5.4 \pm 0.1$. This value, attributed to pK_a^3, is close to p$K_a^3 = 5.6 \pm 0.1$ derived from the absorbance titrations but systematically lower. Therefore, it is possible to speculate that the excited singlet state of the FB $TSPC^{4-}$ is slightly more acidic than ground-state S_0, i.e., $\Delta pK_a^3(S_1-S_0) = pK_a^3(S_1) - pK_a^3(S_0) = -0.2$.

Transitions between different emissive species can also be followed by plotting the pH dependence of the fluorescence spectrum maximum (Figure 7d). Emission of FB $TSPC^{4-}$ also dominates in this case. The peak position of the emission spectrum bears the features of FB fluorescence at low pH (4.0). The obtained pK_a value should be attributed to the formation of DP species since Φ_F of MP species is negligibly small (vide infra). The measured p$K_a^4 = 3.2 \pm 0.1$ is noticeably smaller than 4.6 ± 0.1 found for the ground state (vide supra). The difference between these two values $\Delta pK_a^4(S_1-S_0) = pK_a^4(S_1) - pK_a^4(S_0) = -1.4$ is larger than that obtained for equilibrium of the FB $TSPC^{4-}$ and MP $HTSPC^{3-}$ molecules. The question is whether DP H_2TSPC^{2-} has such an acidic excited singlet S_1 state or the p$K_a^4 = 3.2$ is underestimated due to the domination of emission by FB molecules. This is an open issue that should be studied separately.

Changes in pH induce changes in the relative amplitudes A_i of components in the fluorescence decay kinetics. A redistribution of molecules in the solution over three types of molecules occurs at the various pHs since each of the species has its own distinct decay rate, as shown above. The individual values of pK_a^3 and pK_a^4 for FB/MP and MP/DP equilibria have been found from analysis of pH dependencies of the preexponential factors A_i (Figure 5). The values p$K_a^3 = 3.9 \pm 0.15$ and p$K_a^4 = 3.7 \pm 0.15$ are different from those determined from steady-state fluorescence and absorbance titrations.

The Hill indices are close to unity within experimental error (Table 1) and are similar to those derived from absorption and steady-state fluorescence titrations. However, the values of the relative amplitudes A_i do not completely reflect the relative population of species in the solution, because the different absorbance of the various species should also be taken into account in view of the lack of isobestic points. These measurements should ideally be performed by excitation at the isobestic point of all three species and need to be detected at corresponding isoemissive points in the fluorescence spectra. There are no such points in the present system, as already stated. The obtained set of A_i values as a function of pH allows tracing only the trend in the population of each species with a rather large uncertainty. The contribution into the scatter of the A_i values is given also by the relatively large uncertainty in the three-exponential decay fit as well as by the necessity of taking into account a fourth species at acidic pH. All these factors contribute to the distortion of the relative amplitudes A_i in the decay kinetics.

Fluorescence of Monoprotonated, MP, Species. Whereas the emission spectra and Φ_F of FB $TSPC^{4-}$ and DP H_2TSPC^{2-} can be readily obtained from steady-state fluorescence measurements at extreme alkaline and acidic pH, the fluorescence spectrum and yield of MP species are unknown. The spectrum of each individual species can be reconstructed from time-resolved fluorescence data in a pH range where the corresponding decay components are detected. Favorable pH for reconstruction of the MP molecule spectrum is about 4.0, since the concentration is rather high and the strong component with lifetime $\tau_1 = 8.5$ ns does not dominate in the decay kinetics. For reconstruction of the spectrum the decay kinetics was measured at several wavelengths in the spectral range 600−800 nm. The intensity of emission from each individual species as a function of wavelength $I_i(\lambda)$ is given by eq 3,

$$I_i(\lambda) = \frac{1}{t(\lambda)} \frac{A_i(\lambda)\tau_i}{\sum_{i=1-3} A_i(\lambda)\tau_i} \qquad (3)$$

where $1/[t(\lambda)]$ is a period of time during which the decay kinetics reaches the same peak intensity at all the wavelengths and other values have their usual meaning. The values of $t(\lambda)$ were in the range of several minutes to exclude statistical effects of the photon-counting acquisition system. The calculated spectra for

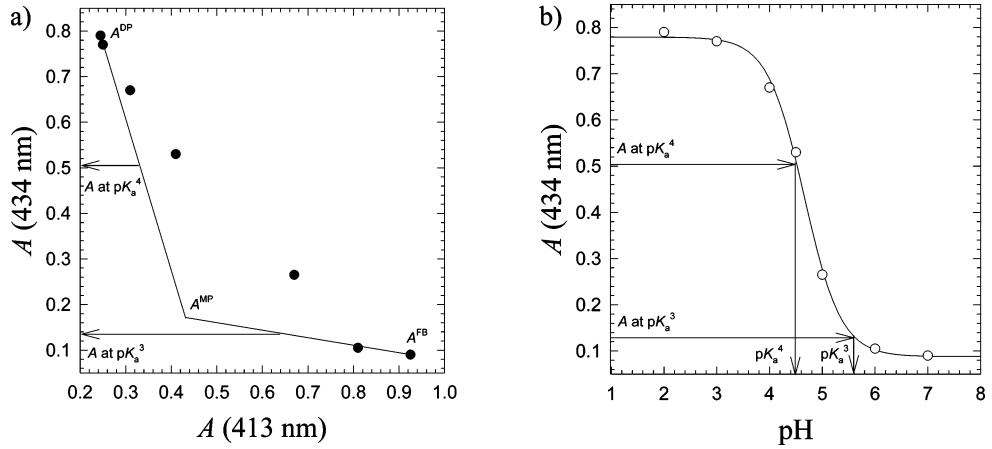

Figure 6. Determination of separate pK_a values for FB ⇄ MP and MP ⇄ DP equilibria: (a) absorbance at 434 nm vs absorbance at 413 nm; (b) absorbance at 434 nm vs pH (see text for details).

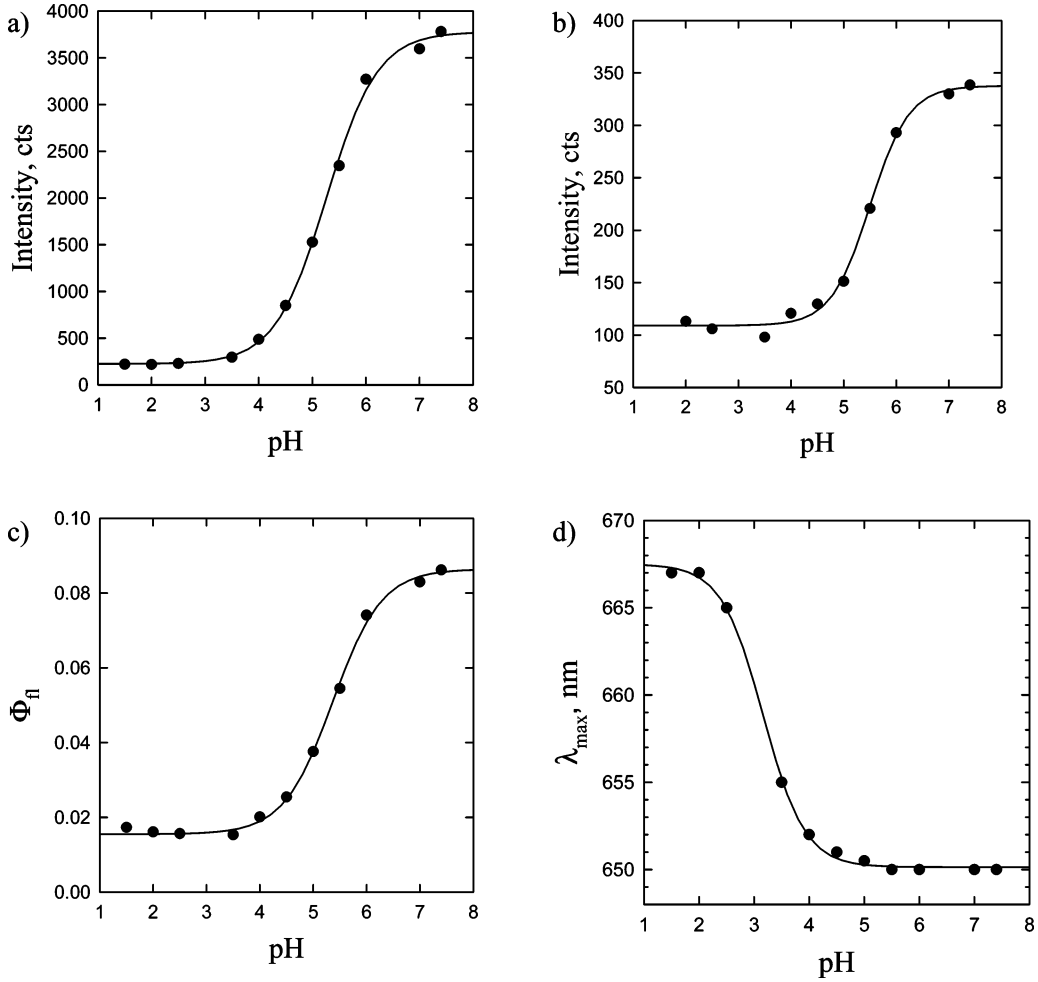

Figure 7. Fluorescence titration curves (a) at $\lambda = 650$ nm; (b) at $\lambda = 715$ nm; (c) of fluorescence quantum yield Φ_F; (d) of fluorescence spectrum λ_{max}.

each emissive species and the total reconstructed spectrum at pH = 4.0 are shown in Figure 8, together with the corresponding steady-state spectrum for comparison.

The contribution from FB emission to the reconstructed spectrum is the largest. The shapes of the various spectra are very similar. DP molecules reveal a red-shifted spectrum with practically the same band half-width. The intensity of the emission from the MP species is about 50 times smaller than that of the DP molecules. The spectrum of MP molecules has a maximum at about the same wavelength as that of DP molecules, but the shape of the spectrum is distinctly different. MP species show one diffuse band with a half-width about twice that of the DP and FB molecules. No vibronic band is observed.

The low fluorescence intensity of $HTSPC^{3-}$ indicates a very low Φ_F since its relative population is of the same order of magnitude as the two other species. A simple approach to calculate Φ_F^{MP}, based on the relative A_i values, cannot be applied because the component relative intensities do not reflect the true relative proportions of the species in the solution (vide supra). However, having two fluorescence spectra measured at

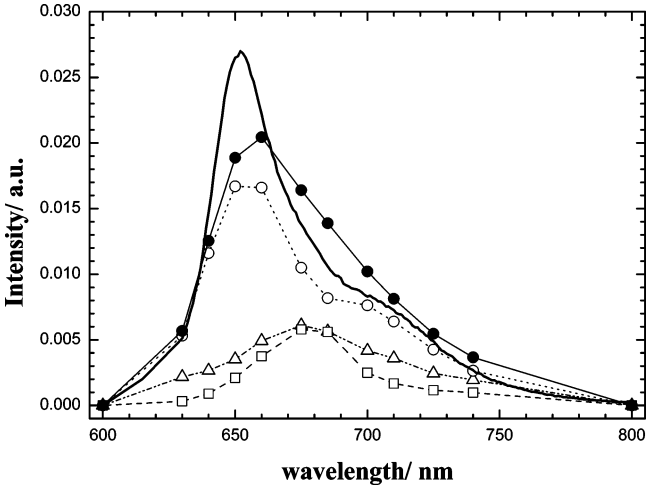

Figure 8. Reconstructed fluorescence spectra at pH = 4.0: (○) FB $TSPC^{4-}$; (Δ) MP $HTSPC^{3-}$ (multiplied by 50); (□) DP H_2TSPC^{2-}; (●) overall spectrum for all three species. Solid line is the steady-state fluorescence spectrum measured at pH = 4.0.

pH = 4.0 (reconstructed from fluorescence decay kinetics and steady-state measurements), it is possible to estimate Φ_F^{MP}.

Thus, $\Phi_F = 0.02$ at pH = 4.0 is the value averaged over three species ($TSPC^{4-}$ with a C_1 contribution, $HTSPC^{3-}$ with a C_2 contribution, and H_2TSPC^{2-} with a C_3 contribution), i.e., $\Phi_F = C_1 \times \Phi_F^{FB} + C_2 \times \Phi_F^{MP} + C_3 \times \Phi_F^{DP}$, where $\Phi_F^{FB} = 0.086$ and $\Phi_F^{DP} = 0.015$, derived from the alkaline and acid edges of the fluorescence quantum yield titration curve (vide supra). On the other hand, the average fluorescence intensity in the spectrum rebuilt from time-resolved fluorescence data is the sum of the intensities due to emission of the three components $I_\Sigma = I^{FB} + I^{MP} + I^{DP}$, and all three are known. From combination of the two equations $\Phi_F^{MP} = (3 \pm 1) \times 10^{-4}$ is derived. In spite of the large uncertainity in this estimation, Φ_F^{MP} is distinctly lower (ca. 1/60) than the value for DP H_4TSPC^{2-}.

Triplet State Properties. The quantum yield for triplet state formation, Φ_T, was determined using singlet oxygen time-resolved phosphorescence and LIOAS. The formation efficiency of the triplet states upon photoexcitation, detected in the whole studied pH range, was found to depend strongly on the protonation state.

Singlet oxygen quantum yield, Φ_Δ, measured by comparison with a standard sample, is given by eq 4,

$$\Phi_\Delta = \Phi_\Delta^{st} \frac{I_\Delta}{I_\Delta^{st}} \frac{f^{st}}{f} \tag{4}$$

where Φ_Δ^{st} is the quantum yield of the singlet oxygen production by the standard, and I_Δ, I_Δ^{st} and f, f^{st} are intensities of $O_2(^1\Delta_g)$ phosphorescence and fractions of the excitation radiation absorbed by the sample and standard solutions, respectively. The intensities I_Δ and I_Δ^{st} were determined from the biexponential decay of the $O_2(^1\Delta_g)$ phosphorescence as described earlier.[24] The singlet oxygen phosphorescence lifetime was found to be $\tau_\Delta = 3.7 \pm 0.3$ μs for all samples.

The Φ_T value estimated from Φ_Δ affords a lower limit of Φ_T, since $\Phi_\Delta = f_\Delta^T \Phi_T$, where f_Δ^T is the fraction of quenched triplet states yielding $O_2(^1\Delta_g)$. In alkaline solutions for FB $TSPC^{4-}$, $\Phi_\Delta = 0.41 \pm 0.05$, and at acidic pH the value for H_2TSPC^{2-} is $\Phi_\Delta = 0.12 \pm 0.02$.

Φ_T was also calculated using the fraction of heat released during the formation of the lowest T_1 state, α_1, measured with

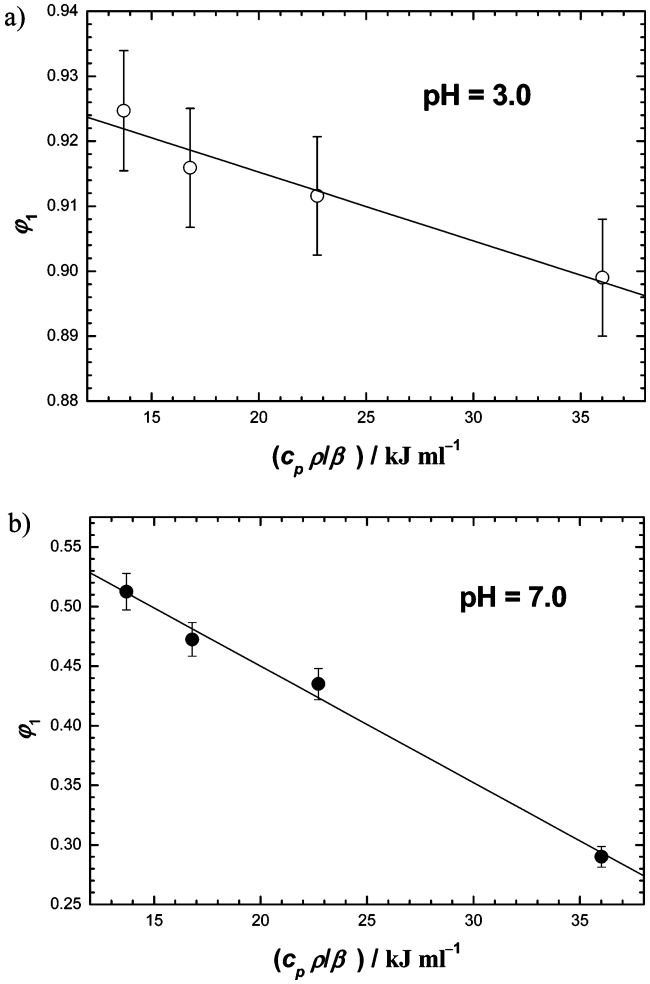

Figure 9. First amplitude of the biexponential fitting versus the ratio of thermoelastic parameters (eq 2) for (a) DP and (b) FB forms of 5,10,15,20-tetrakis(4-sulfonatophenyl)chlorin with BCP as calorimetric reference.

LIOAS (eq 5[26]),

$$\Phi_T = \frac{E_\lambda}{E_T}\left(1 - \alpha_1 - \frac{\Phi_F E_F}{E_\lambda}\right) \tag{5}$$

where α_1 is the heat released upon formation of the triplet state (eq 1, intercepts in Figure 9), $E_\lambda = 224.7$ kJ mol^{-1}, E_T, and E_F are the molar energy of the laser pulse (532 nm), the lowest triplet energy, and the fluorescence energy, respectively. The α_1 values were 0.936 and 0.646 for H_2TSPC^{2-} and $TSPC^{4-}$, respectively. $E_F = 179$ and 184 kJ mol^{-1} for H_2TSPC^{2-} and $TSPC^{4-}$ were calculated from the respective peak fluorescence wavelengths.

To estimate E_T it was assumed that sulfonation does not affect the excited-state energy noticeably.[41] We also noticed that the shifts in the peak position of the phosphorescence spectra at 77 K and room temperature for tetra-*meso*-aryl-substituted porphyrins and chlorins are very small. Thus, $E_T = 133.8$ kJ mol^{-1} was estimated for FB $TSPC^{4-}$ as found for TPC at 77 K.[34]

The calculated $\Phi_T = 0.48 \pm 0.05$ is in reasonable agreement with $\Phi_T = 0.41$ estimated from $O_2(^1\Delta_g)$ photosensitization (vide supra). Provided that the energy difference −5.4 kJ mol^{-1} between DP porphyrin is the same for chlorin,[34,41] $E_T = 116.6$ kJ mol for H_2TSPC^{2-} is calculated. $\Phi_T = 0.10 \pm 0.02$ for H_2TSPC^{2-} is in excellent agreement with the estimation $\Phi_T = \Phi_\Delta = 0.12$. This supports the above suggestion regarding a unity efficiency for $O_2(^1\Delta_g)$ production upon triplet quenching.

TABLE 2: Photophysical Properties of 5,10,15,20-Tetrakis(4-sulfonatophenyl)chlorin as a Function of Protonation State[a]

protonation state	Φ_F	Φ_Δ	Φ_T	Φ_{IC}	$k_F/10^7\ s^{-1}$	$k_{ISC}/10^7\ s^{-1}$	$k_{IC}/10^7\ s^{-1}$	τ_F/ns	$\Delta_T V$/Å^3
$TSPC^{4-}$ (FB)	0.086 ± 0.005	0.41 ± 0.05	0.48 ± 0.05	0.50± 0.06	1.01	4.82	5.94	8.5 ± 0.15	−8.9
				(0.43) ± 0.06		(5.65)	(5.11)		(−7.6)
$HTSPC^{3-}$ (MP)	0.0003 ± 0.0001		–		0.052			0.5 ± 0.15	
H_2TSPC^{2-} (DP)	0.015 ± 0.005	0.12 ± 0.02	0.10 ± 0.02	0.87 ± 0.03	0.43	3.43	24.7	3.5 ± 0.20	−3.3
				(0.89) ± 0.03		(2.86)	(25.3)		(−4.0)

[a] The values of rate constants k_F, k_{ISC}, and k_{IC} are given with an accuracy of 10%, and those of structural volume changes $\Delta_T V$ with an accuracy of 20%. Values of Φ_{IC}, k_{ISC}, k_{IC}, and $\Delta_T V$ were calculated using either $O_2(^1\Delta_g)$ luminescence or LIOAS data. The latter are given in parentheses.

The Φ_T drop with pH decrease parallels that found for Φ_F and indicates that formation of H_2TSPC^{2-} leads to a strong increase in the efficiency of radiationless deactivation through internal $S_1 \rightarrow S_0$ conversion, with a k_{IC} that strongly increases as compared with that for $TSPC^{4-}$.

The values $\tau_T = 1.9 \pm 0.1$ μs and 2.0 ± 0.1 μs for $TSPC^{4-}$ at pH =7.0 and for H_2TSPC^{2-} at pH = 3.0, respectively, in air equilibrated buffer solution, obtained from both the treatment of the $O_2(^1\Delta_g)$ phosphorescence kinetics and transient triplet−triplet absorption decays were the same within experimental error. The roughly estimated triplet state quenching rate constant by molecular oxygen is $k_T = 1/(\tau_T[O_2]) = 1.9 \times 10^9\ M^{-1}\ s^{-1}$, identical to the value for the corresponding FB and DP porphyrin species.[19,24]

Efficiency of Nonradiative Deactivation of Excited States. Data analysis (Table 2) shows that for both $TSPC^{4-}$ and H_2TSPC^{2-} internal conversion $S_1 \rightarrow S_0$ is the main channel of deactivation. About one-half of the excited $TSPC^{4-}$ molecules deactivate through this channel, as indicated by both the value of $\Phi_{IC} = 1 - \Phi_F - \Phi_T$, and the corresponding rate constant k_{IC}. Internal conversion accounts for about 90% of deactivation in H_2TSPC^{2-}. On the contrary, Φ_{ISC} decreases from 45% to about 10% from $TSPC^{4-}$ to H_2TSPC^{2-}. Comparison of the corresponding rate constants k_{IC} and k_{ISC} indicates that this decrease is mainly due to a large increase in k_{IC}. This rate constant increases five times in going from $TSPC^{4-}$ to H_2TSPC^{2-}, and no other channel can compete with it. Taken together, IC and ISC are the main deactivation channels. The radiative transitions explain less than 10% and 2% of deactivation, respectively. The ratio of Φ_F^{FB}/Φ_F^{DP} is not equal to that of emission rate constants. This means that decrease in the Φ_F is mainly due to a dramatic enhancement of the internal conversion rate rather than to a strong decrease in emission rate constant k_F upon formation of H_2TSPC^{2-}.

The energy gap between the S_1 and ground S_0 states is about the same as for the porphyrin counterpart.[19] Therefore, a simple energy gap factor is unable to explain the substantially larger value of IC for $TSPC^{4-}$ and the large increase in H_2TSPC^{2-}. One of the reasons for such a behavior should lie in the structural factors inducing a molecular symmetry lowering upon reduction of one of the pyrrole rings. Thus, either different molecular orbitals account for the electronic transition or changes in the configuration interaction take place.

As for the triplet states, it was earlier proposed that different molecular electronic orbitals are involved in the electronic configuration of the lowest triplet states in tetraphenylporphyrin and its reduced counterpart.[42] The b_{1u} orbital (in D_{2h} symmetry notation) participates in the formation of lowest T_1 state one-electron configuration in the porphyrins, whereas it is formed with an a_u orbital in the case of the chlorins. Once formed, these triplet states are very similar in both energy level and reactivity. However, the values of k_{ISC} for these two types of molecules seem to be very different. Thus, $k_{ISC} = 5 \times 10^7\ s^{-1}$ for FB chlorin and $6 \times 10^7\ s^{-1}$ for FB porphyrin,[19] but k_{ISC} decreases for DP chlorin to ca. $3 \times 10^7\ s^{-1}$ and increases for DP porphyrin up to ca. $1.5 \times 10^8\ s^{-1}$.[19,24]

Enhanced flexibility of the reduced macrocycle compared to that of the porphyrin facilitates the motion along the potential energy surface leading to the conformational substates with increased probability of nonradiative deactivation of the excited states.[36] The importance of these factors is discussed extensively for tetrapyrrolic compounds with a high degree of nonplanar distortions.[43−45] One of the prominent examples of such influence is the diprotonation of the porphyrin molecule which forces the molecule to adopt a saddle shape conformation with extensive perturbation of the rates and yields of excited-state deactivation. The perturbations correlate with the extent of deviation from the macrocycle planarity.[35,46] Changes in the level of saturation of the π-conjugation system of the chlorin macrocycle due to the pyrrole reduction seem to enormously increase the molecular flexibility, leading to an increase in the internal conversion rate.

Structural Volume Changes. The only structural difference between the molecules of $TSPC^{4-}$ and $TSPP^{4-}$ is the reduction of the pyrrole ring. It is of interest to test whether structural alterations of the tetrapyrrolic macrocycle have any influence on the structural volume change upon triplet state formation, $\Delta_T V$. So far, it has been found that the type of *meso*-aryl-substituents has almost no influence on the $\Delta_T V$ value. A contraction of 16−18 Å^3 and 4−5 Å^3 upon triplet formation of FB and DP forms was measured independently of substitution.[19]

Two sets of LIOAS measurements were performed in the temperature range 10−25 °C for $TSPC^{4-}$ at pH = 7.0 and for H_2TSPC^{2-} at pH = 3.0 and 7.0.

The plots of the fractional amplitudes of the prompt heat release φ_1 upon triplet state formation are shown in Figure 9. The corresponding plots of fractional amplitudes φ_2 for the subsequent expansion due to the decay of the triplet state revealed similar results (with opposite sign of the slope), but the data scatter was very high (data not shown).

A value $\Phi_T\ \Delta_T V = -0.24$ mL mol^{-1} was found for DP H_2TSPC^{2-} from the slope in Figure 9. Thus, with the average value of $\Phi_T = 0.11$, a contraction $\Delta_T V = -2.2$ mL mol^{-1} (−3.7 Å^3) was calculated, close to those measured for DP forms of several porphyrins in aqueous solution.[19] Thus, the interaction of the highly distorted macrocycle with the hydrated water shell is of the same order of magnitude for both porphyrin and chlorin molecules.

A similar procedure afforded $\Phi_T\ \Delta_T V = -2.20$ mL mol^{-1} for FB $TSPC^{4-}$. With $\Phi_T = 0.45$ a contraction $\Delta_T V = -5.0$ mL mol^{-1} (−8.3 Å^3) was calculated, about one-half of that found for the FB porphyrins, although the trend upon going from DP to FB parallels that reported for porphyrins.

Following the model given in the preceding paper,[19] the contraction upon excitation should be due to the fact that the two free nitrogen atoms in the macrocycle are more strongly hydrogen bonded with the surrounding water molecules in the triplet state than in the ground state. We find now that these

intermolecular interactions should be about 50% weaker for the reduced macrocycle. Such a weakening is likely to be due to the increased flexibility of the reduced macrocycle. It has been shown that the potential energy surface of conformational rearrangement is quite different for the various types of tetrapyrrolic macrocycles.[47] The gradient of this surface along the coordinates that relate to distance to the center nitrogen is smaller for a chlorin than for a porphyrin. The shallowness of the conformational energy surface along this and other atomic coordinates is what is meant by increased molecular flexibility.[35,47] We assume that for the more flexible chlorin the molecular rearrangement upon photoexcitation to adopt a minimum energy equilibrium conformation occurs noticeably by intramolecular conformational rearrangement and the intermolecular hydrogen bonding with the surrounding water molecules is less involved. On the contrary, for the less flexible porphyrin, the contribution from intermolecular interactions increases. This is also reflected in the fact that dimers appear in the porphyrin at a lower concentration than in the equally *meso*-substituted chlorin (compare present data with data for $TSPP^{4-}$ [19]). Thus, it is possible to propose that $\Delta_T V$ reflects to some extent the molecular flexibility and in several cases serves as its measure.

Conclusions

The acid−base equilibria in 5,10,15,20-tetrakis(4-sulfonatophenyl)chlorin have been studied in aqueous solution. The reduction of the pyrrole ring in the tetrapyrrolic macrocycle strongly influences both FB/MP and MP/DP species equilibria. Values of $pK_a^3 = 5.6 \pm 0.1$ and $pK_a^4 = 4.6 \pm 0.1$, respectively, are obtained. Therefore, FB $TSPC^{4-}$ can be considered as more basic and DP H_2TSPC^{2-} as more acidic than the corresponding forms of the equally substituted porphyrin. Protonation of the 4-sulfonatophenyl groups occurs in strong acidic solutions. The photophysical properties of all the ionic forms of the chlorin are strongly influenced by an enhanced rate of radiationless internal conversion $S_1 \rightarrow S_0$. Thus, about 50% of FB molecules and up to 90% of DP molecules are deactivated through this channel. Such an increase in the radiationless transition rate is explained by an increased conformational flexibility of the reduced tetrapyrrolic macrocycle (i.e., dihydroporphyrin or chlorin) as compared to the corresponding porphyrin. Support for this hypothesis is found in the structural volume changes measured with laser-induced optoacoustic spectroscopy. The contraction of 8.3 Å^3 per molecule upon triplet state formation is about one-half of that for the corresponding porphyrin. Intramolecular structural rearrangements of the macrocycle to adopt a minimum energy conformation are favored in the chlorin. Solute−solvent interactions are expected to be more involved in the more rigid porphyrin macrocycle, at the expense of intramolecular conformational rearrangements. The DP forms of porphyrin and chlorin have a similar conformational flexibility (for both $\Delta_T V = -4 \pm 1$ Å^3 per molecule), and both of them show strong radiationless internal $S_1 \rightarrow S_0$ conversion rates.

Acknowledgment. M.M.K. acknowledges DAAD for financial support. We are grateful to Andrea Keil-Block, Gudrun Klihm, Gul Koç-Weier, and Dagmar Lenk, for their able technical assistance and to Drs. Aba Losi and Edwin Yeow for valuable discussions.

Abbreviations

DP	diprotonated form
FB	free base
LIOAS	laser-induced optoacoustic spectroscopy
MP	monoprotonated form
$TSPC^{4-}$	free base 5,10,15,20-tetrakis(4-sulfonatophenyl)chlorin
$TSPP^{4-}$	5,10,15,20-tetrakis(4-sulfonatophenyl)porphin
Φ_F, Φ_T, Φ_Δ	fluorescence, triplet, and singlet molecular oxygen production quantum yield

References and Notes

(1) Spikes, J. D.; Straight, R. C. In *Photodynamic Therapy of Tumors and Other Diseases*; Jori, G.; Perria, C., Eds.; Libreria Progetto Editore: Padova, 1985; pp 45−53.
(2) Bonnett, R. *Chemical Aspect of Photodynamic Therapy*; Gordon and Breach Science Publishers: Amsterdam, 2000.
(3) Vaupel, P. V.; Frinak, S.; Bicher, H. I. *Cancer Res.* **1981**, *41*, 2008−2013.
(4) Albers, C.; van den Kerkhoff, W.; Vaupel, P.; Müller-Klieser, W. *Respir. Physiol.* **1981**, *45*, 273−285.
(5) Tannock, I. F.; Rotin, D. *Cancer Res.* **1989**, *49*, 4373−4384.
(6) Gerweck, L. E.; Seetharaman, K. *Cancer Res.* **1996**, *56*, 1194−1198.
(7) Wike-Hooley, J. L.; Haverman, J.; Reinhold: H. S. *Radiother. Oncol.* **1984**, *2*, 343−366.
(8) Pottier, R. H.; Kennedy, J. C.; Chow, Y. F. A.; Cheung, F. *Can. J. Spectrosc.* **1988**, *33*, 57−62.
(9) Barrett, A. J.; Kennedy, J. C.; Jones, R. A.; Nadeau, P.; Pottier, R. H. *J. Photochem. Photobiol. B: Biol.* **1990**, *6*, 309−323.
(10) Čunderlikova, B.; Gangeskar, L.; Moan, J. *J. Photochem. Photobiol. B: Biol.* **1999**, *53*, 81−90.
(11) Čunderlikova, B.; Bjørklund, E. G.; Pettersen, E. O.; Moan, J. *J. Photochem. Photobiol. B: Biol.* **2001**, *74*, 246−252.
(12) Zhang, J. Z.; Oneil, R. H.; Evans, J. E. *Photochem. Photobiol.* **1994**, *60*, 301−309.
(13) Ojadi, E. C. A.; Linschitz, H.; Gouterman, M.; Walter, R. I.; Lindsey, J. S.; Wagner, R. W.; Droupadi, P. R.; Wang, W. *J. Phys. Chem.* **1993**, *97*, 13192−13197.
(14) Ostler, R. B.; Scully, A. D.; Taylor, A. G.; Gould, I. R.; Smith, T. A.; Waite, A.; Phillips, D. *Photochem. Photobiol.* **2000**, *71*, 397−404.
(15) Dedic, R.; Molnar, A.; Korinek, M.; Svoboda, A.; Psencik, J.; Hala, J. *J. Lumin.* **2004**, *108*, 117−119.
(16) Phillips, J. N. In *Comprehensive Biochemistry*; Florkin, M.; Stotz, E. H., Eds.; Elsevier: Amsterdam, 1963; Vol. 9, pp 34−72
(17) Maman, L.; Brault, D. *Biochim. Biophys. Acta* **1998**, *1414*, 31−42.
(18) Dairou, J.; Vever-Bizet, C.; Brault, D. *Photochem. Photobiol.* **2002**, *75*, 229−236.
(19) Gensch, T.; Viappiani, C.; Braslavsky, S. E. *J. Am. Chem. Soc.* **1999**, *121*, 10573−10582.
(20) Losev, A. P.; Nichiporovich, I. N.; Bachilo, S. M.; Egorova, G. D.; Volkovich, D. I.; Solov'ev, K. N. *J. Appl. Spectrosc.* **1995**, *62*, 311 (translation from Russian).
(21) Holzwarth, A. R.; Lehner, H.; Braslavsky, S. E.; Schaffner, K. *Liebigs Ann. Chem.* **1978**, 2002−2017.
(22) Martínez, G.; Bertolotti, S. G.; Zimerman, O. E.; Mártire, D. O.; Braslavsky, S. E.; García, N. A. *J. Photochem. Photobiol. B: Biol.* **1993**, *17*, 247−255.
(23) Yruela, I.; Churio, M. S.; Gensch, T.; Braslavsky, S. E.; Holzwarth, A. R. *J. Phys. Chem.* **1994**, *98*, 12789−12795.
(24) Gensch, T.; Braslavsky, S. E. *J. Phys. Chem. B* **1997**, *101*, 101−108.
(25) Schmidt, P.; Gensch, T.; Remberg, A.; Gärtner, W.; Braslavsky, S. E.; Schaffner, K. *Photochem. Photobiol.* **1998**, *68*, 754−761.
(26) Gensch, T.; Viappiani, C.; Braslavsky, S. E. In *Encyclopedia of Spectroscopy and Spectrometry*; Tranter, G. E.; Holmes J. L., Eds.; Academic Press: San Diego, 1999; pp 1124−1132.
(27) Malkin, S.; Churio, M. S.; Shochat, S.; Braslavsky, S. E. *J. Photochem. Photobiol. B: Biol.* **1994**, *23*, 79−85.
(28) Churio, M. S.; Angermund, K. P.; Braslavsky, S. E. *J. Phys. Chem.* **1994**, *98*, 1776−1782.
(29) Peters, K. S.; Snyder, G. J. *Science* **1988**, *241*, 1053−1057.
(30) Small, J. R. In *Numerical Computer Methods*; Brand, L.; Johnson M. L., Eds.; Academic Press: San Diego, 1992; Vol. 210, pp 505−521.
(31) Rudzki, J. E.; Goodman, J. L.; Peters, K. S. *J. Am. Chem. Soc.* **1985**, *107*, 7849−7854.
(32) Rothberg, L. J.; Simon, J. D.; Bernstein, M.; Peters, K. S. *J. Am. Chem. Soc.* **1983**, *105*, 3464−3468.
(33) Pasternack, R. F.; Huber, P. R.; Boyd, P.; Engasser, G.; Francesconi, L.; Gibbs, E.; Fasella, P.; Venturo, G. C.; deC. Hinds, L. *J. Am. Chem. Soc.* **1972**, *94*, 4511−4517.

(34) Borissevich, E. A.; Egorova, G. D.; Knukshto, V. N.; Solov'ev, K. N. *Opt. Spectrosk.* **1986**, *60*, 742.

(35) Cheng, B.; Munro, O. Q.; Marques, H. M.; Scheit, W. R. *J. Am. Chem. Soc.* **1997**, *119*, 10732−10742.

(36) Artemenko, A. I. *Reference Book on Chemistry*; Vusshaya shkola: Moscow, 1990 (in Russian).

(37) Kruk, N. N.; Parkhots, O. P.; Ivashin, N. V. *J. Appl. Spectrosc.* **2001**, *68*, 924−929.

(38) Gnedin, B. G.; Schukina, M. V.; Morozov, V. V.; Berezin, B. D.; Semeikin, A. S. *J. Appl. Spectrosc.* **1984**, *41*, 441.

(39) (a) Bernstein, I. Y.; Kaminsky, Y. L. *Spectrophotometric Analysis in Organic Chemistry*; Khimiya: Leningrad, 1986 (in Russian). (b) A similar method was proposed by Polster: Polster, J. *Talanta* **1984**, *31*, 113−116.

(40) Marshall, A. G. *Biophysical Chemistry: Principles, Techniques and Applications*; John Wiley and Sons: New York, 1978.

(41) Knyukshto, V. N.; Solov'ev, K. N.; Egorova, G. D. *Biospectroscopy* **1998**, *4*, 121−133.

(42) Sapunov, V. V.; Solov'ev, K. N.; Tsvirko, M. P. *J. Appl. Spectrosc.* **1974**, *21*, 667.

(43) Senge, M. O. *J. Photochem. Photobiol. B: Biol.* **1992**, *16*, 3−36.

(44) Barkigia, K. M.; Nurco, D. J.; Renner, M. W.; Melamed, D.; Smith, K. M.; Fajer, J. *J. Phys. Chem. B* **1998**, *102*, 322−326.

(45) Shelnutt, J. A.; Song, X.; Ma, J.; Jia, S.; Jentzen, W.; Medforth, C. *Chem. Soc. Rev.* **1998**, *27*, 31−42.

(46) Chirvony, V. S.; van Hoek, A.; Galievsky, V. A.; Sazanovich, I. V.; Schaafsma, T. J.; Holten, D. *J. Phys. Chem. B* **2000,** *104*, 9909−9917.

(47) Stolzenberg, A. M.; Stershic, M. T. *J. Am. Chem. Soc.* **1988**, *110*, 6391−6402.